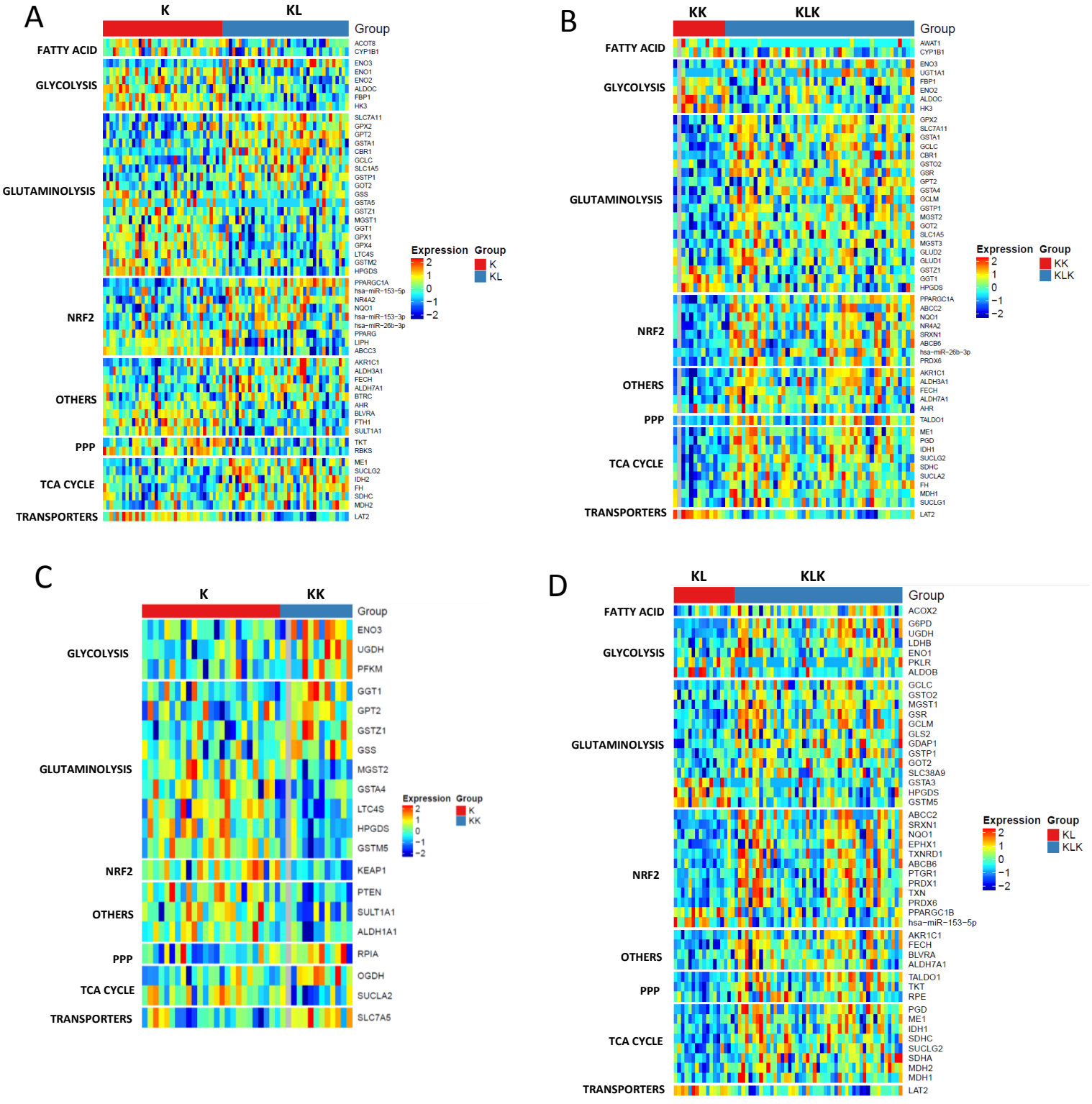

Figure S1. KRAS-mutant tumors with functional inactivation of LKB1 (KL tumors) and a KEAP1 co-mutation (KLK tumors) exhibit evidence of metabolic reprograming and adaptation to oxidative and energetic stress. **(A)** Heatmap depicting mRNA expression levels of significantly associated genes selected for the indicated pathways in K subset compared with KL **(B),** KK subset compared with KLK **(C),** K subset compared with KK or **(D)** KK compared with KLK. GSEA shows enrichment of gene expression signatures in K subset compared with KL subset, **(D)** or KL subset compared with KLK subset.

A

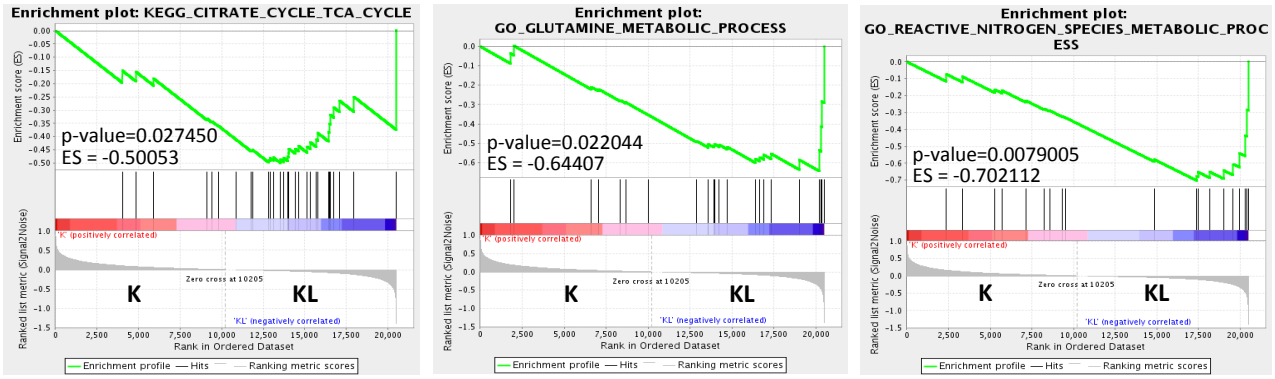

B

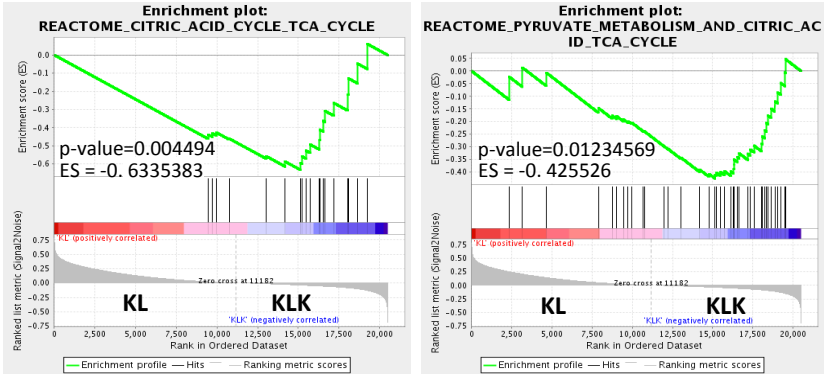

C

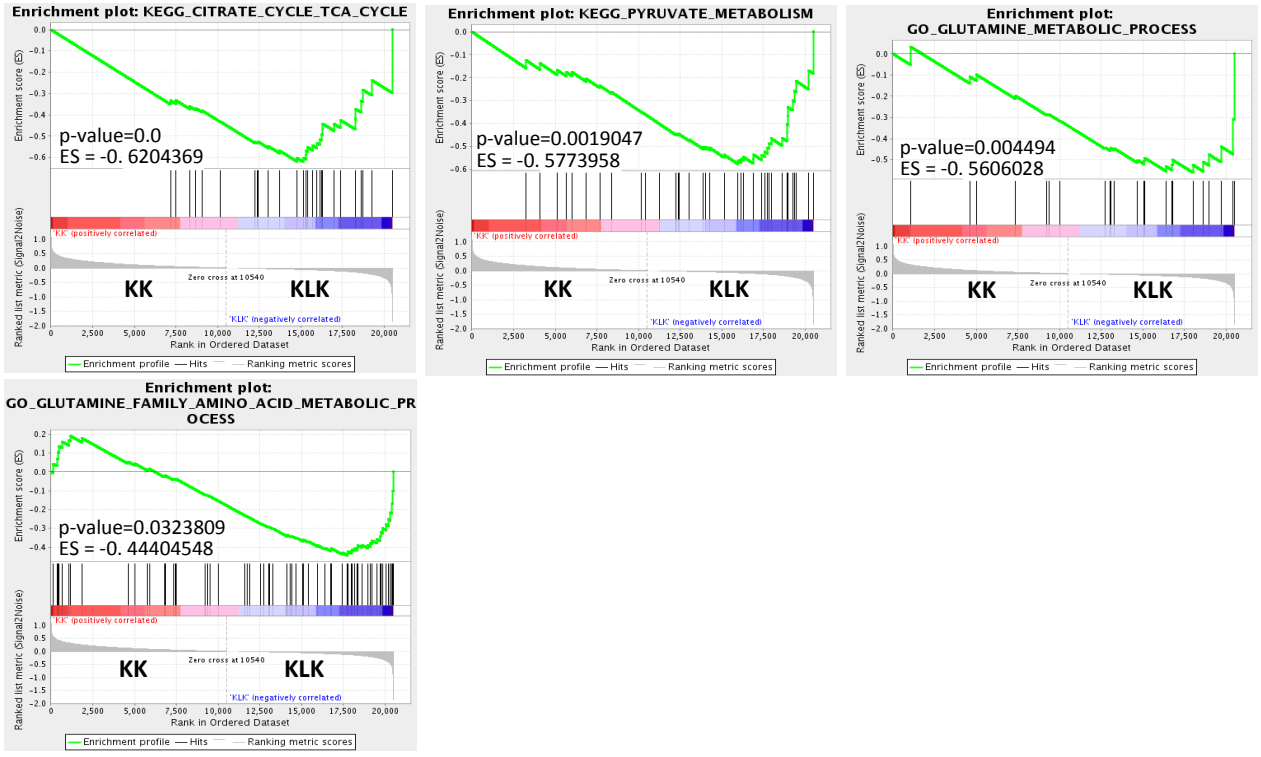

Figure S2. KRAS-mutant tumors with functional inactivation of LKB1 (KL tumors) and a KEAP1 co-mutation (KLK tumors) exhibit evidence of metabolic reprograming and adaptation to oxidative and energetic stress. **(A)** GSEA shows enrichment of gene expression signatures in K subset compared with KL subset, **(B)** KL subset compared with KLK subset **(C)**, or KK subset compared with KLK subset. P-value < 0.05.

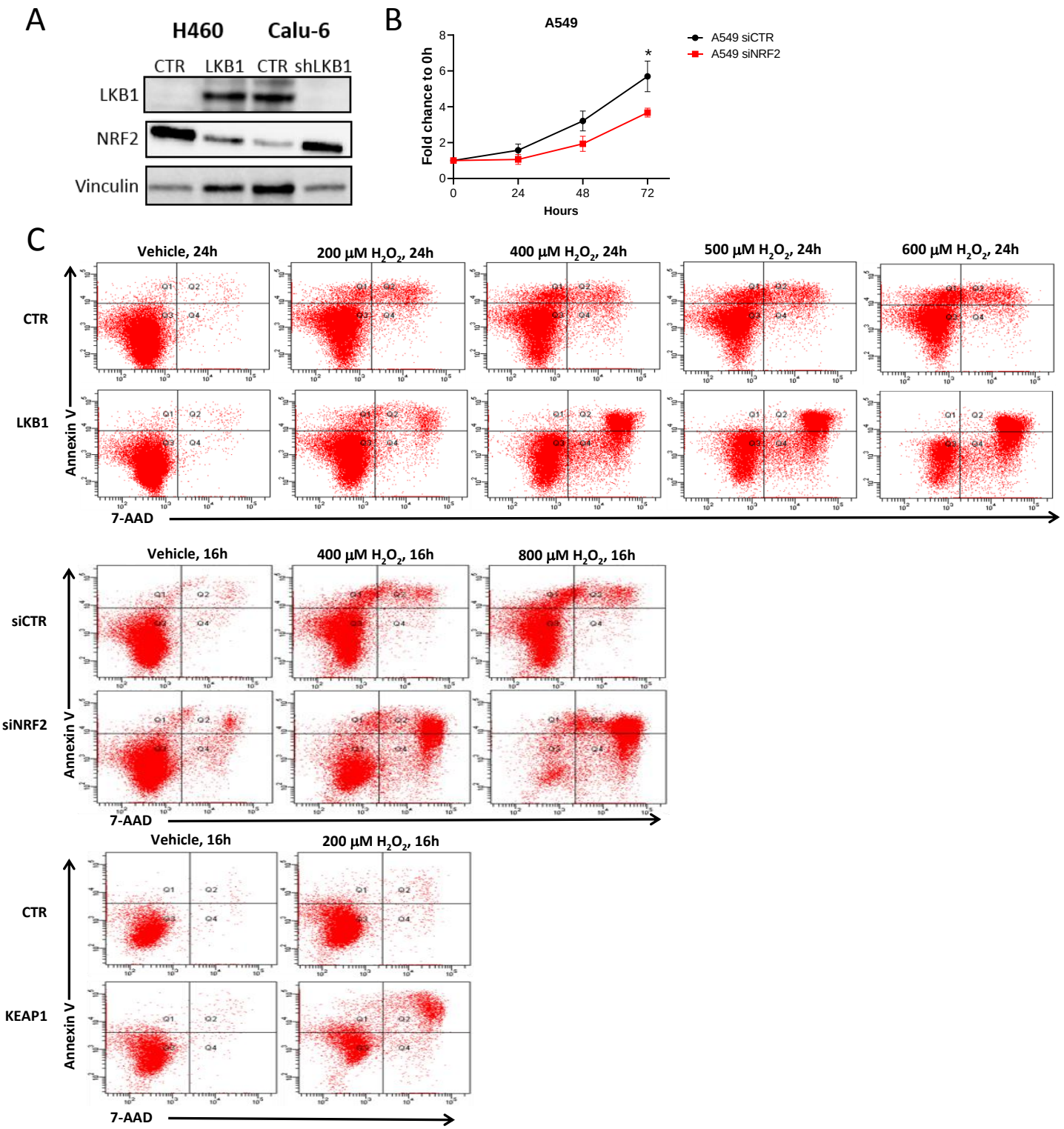

Figure S3. (A) Expression of LKB1 and NRF2 after stable expression of LKB1 or silencing by shLKB1 in A549, Calu-6, and H460 cell lines. Vinculin was used as a loading control. **(B)** Cell proliferation was assessed using cell counting in NRF2-knockdown A549 cells compared with vector control cells (n = 3; mean of three independent experiments are shown in the graph). **(C)** Apoptosis in A549 cells at 24 hours after treatment with 200µM, 400µM, 500µM, and 600µM H_2O_2 in LKB1-overexpression clones, at 16 hours after treatment with 400µM and 800µM H_2O_2 in NRF2-knockdown clones, and at 16 hours after treatment with 200µM H_2O_2 in KEAP1 clones compared with vector control cells, determined by PE-conjugated Annexin-V/7-AAD staining and flow cytometry. *$P \leq 0.05$.

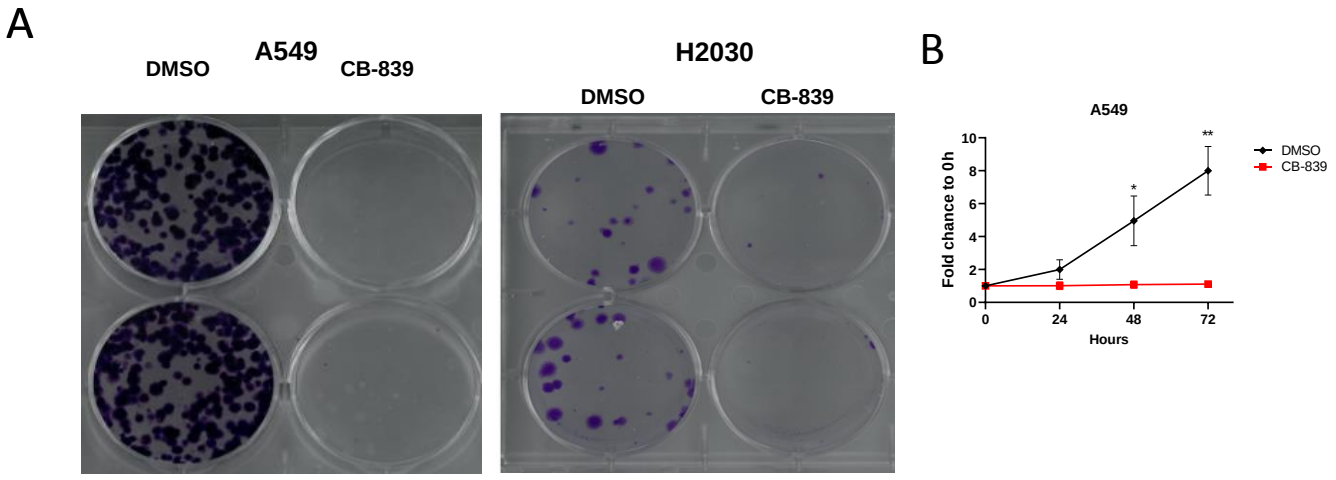

Figure S4. (A) Images of the colonies formed from A549 and H2030 cells after treatment with 1µM CB-839. A representative experiment from three or more experiments is shown. **(B)** Cell proliferation, assessed by cell counting, in A549 cells after treatment with 1µM CB-839 (n = 4; mean of 4 independent experiments are shown in the graph). Data are presented as mean ± standard error of the mean (error bars). Statistical significance: **P ≤ 0.01 and *P ≤ 0.05.

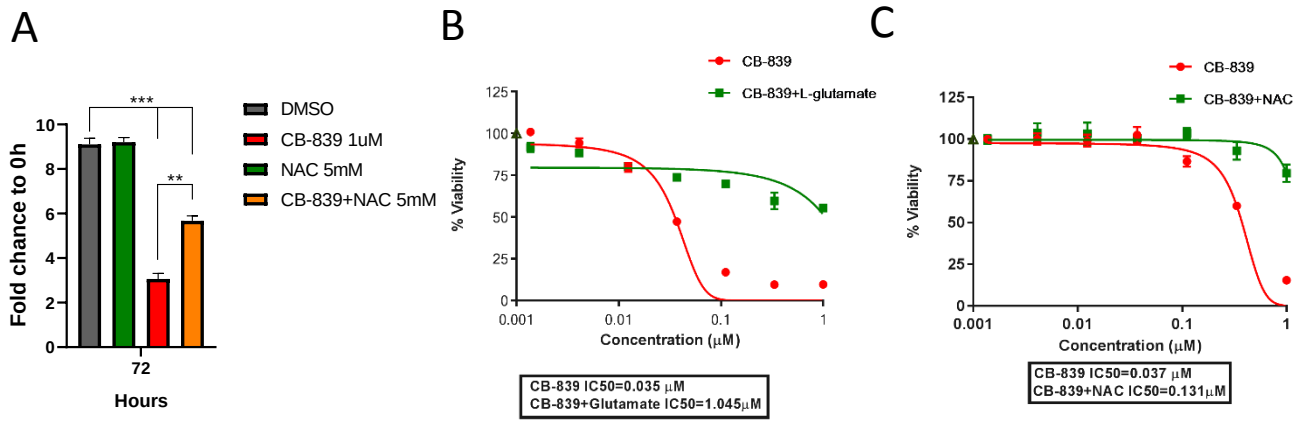

Figure S5. (A) Cell proliferation rate by cell counting method after 72 hours of 1µM CB-839 and NAC (n=3; mean of 3 independent experiments are shown in the graph). **(B)** Dose response curve of A549 cells after treatment with 1µM CB-839 and NAC or **(C)** glutamate (A representative experiment is shown). All data are presented as mean ± standard error of the mean (error bars). IC50, half-maximal inhibitor concentration. ***P ≤ 0.001 and **P ≤ 0.01.

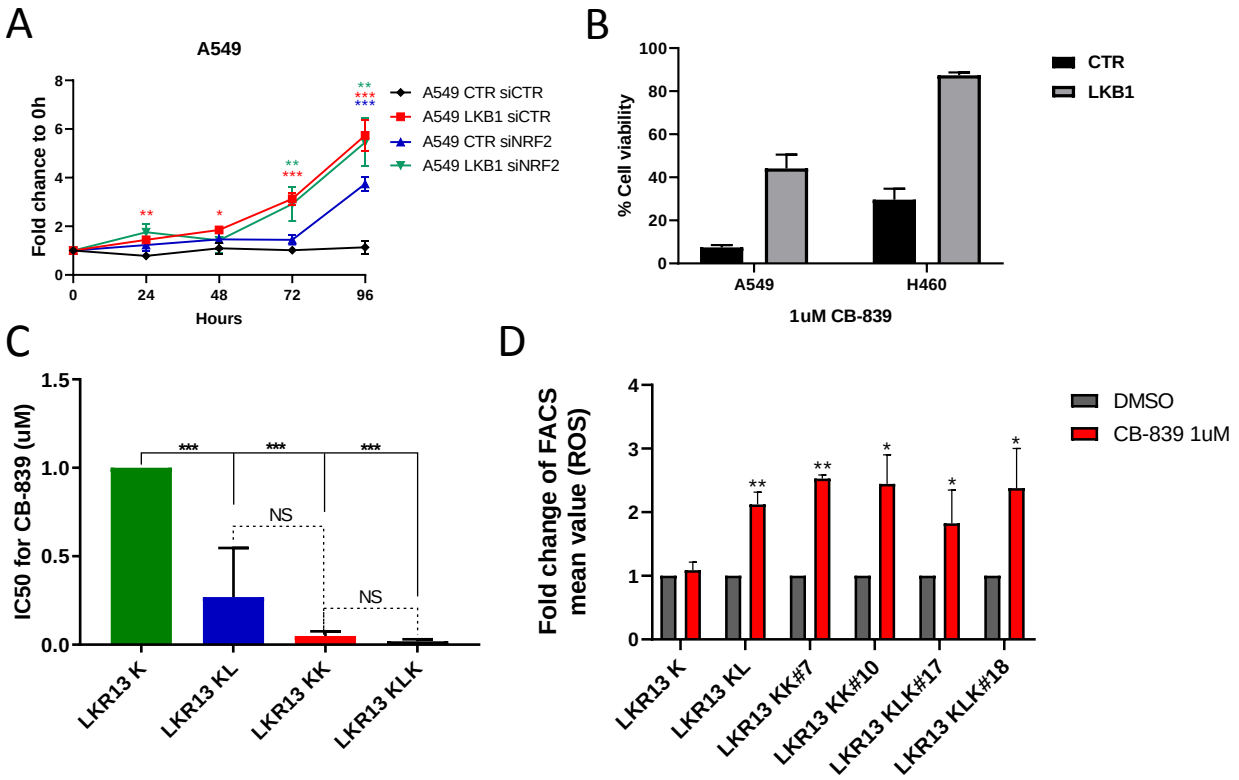

Figure S6. LKB1 and KEAP1 loss contribute to high sensitivity to CB-839. **(A)** Cell proliferation assessed by cell counting in isogenic LKB1 pairs of A549 cells with or without NRF2 knockdown after treatment with 1μM CB-839 (n = 4; mean of four independent experiments are shown in the graph). **(B)** Cell viability after 72 hours of treatment with 1μM CB-839 in isogenic LKB1 pairs of A549 and H460 cells (n = 3; mean of three independent experiments are shown in the graph). **(C)** Summary of IC50 concentrations CB-839 in LKR13 isogenic pairs (n = 4; mean of four independent experiments are shown in the graph). **(D)** Intracellular reactive oxygen species (ROS) levels were monitored using CellROX Deep Red and flow cytometry after 48 hours of treatment with 1μM CB-839 (n = 3; mean of three different experiments are shown in the graph). All data are presented as mean ± standard error of the mean (error bars). IC50, half-maximal inhibitor concentration. ***P ≤ 0.001, **P ≤ 0.01 and *P ≤ 0.05.

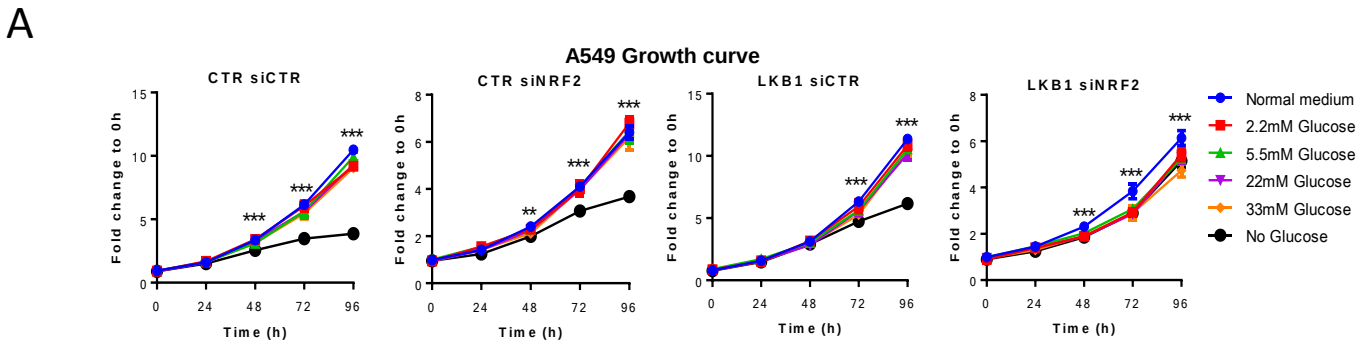
A
A549 Growth curve
CTR siCTR
CTR siNRF2
LKB1 siCTR
LKB1 siNRF2
Fold change to 0h
Time (h)
Normal medium
2.2mM Glucose
5.5mM Glucose
22mM Glucose
33mM Glucose
No Glucose

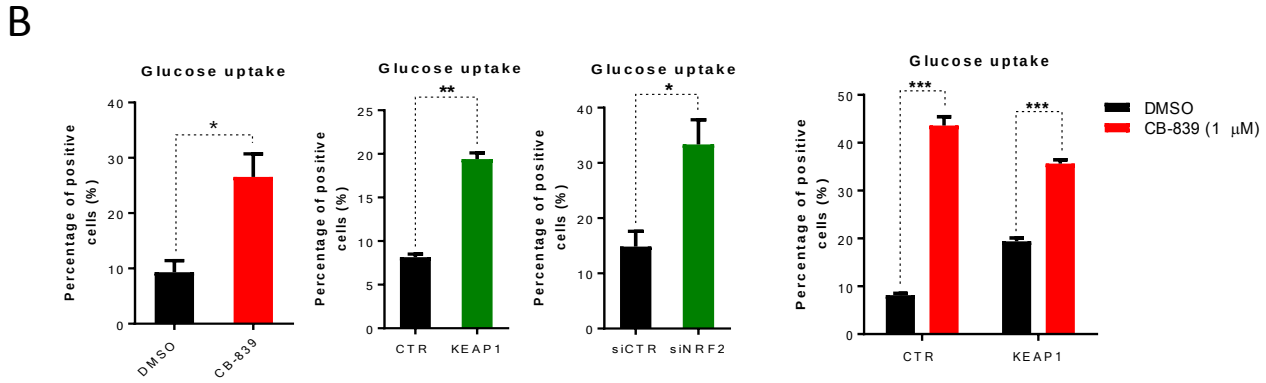
B
Glucose uptake
Percentage of positive cells (%)
DMSO
CB-839
CTR
KEAP1
siCTR
siNRF2
DMSO
CB-839 (1 μM)

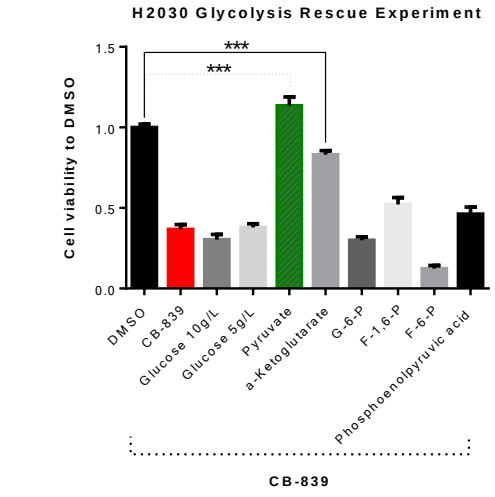
C
H2030 Glycolysis Rescue Experiment
Cell viability to DMSO
DMSO
CB-839
Glucose 10g/L
Glucose 5g/L
Pyruvate
a-Ketoglutarate
G-6-P
F-1,6-P
F-6-P
Phosphoenolpyruvic acid
CB-839

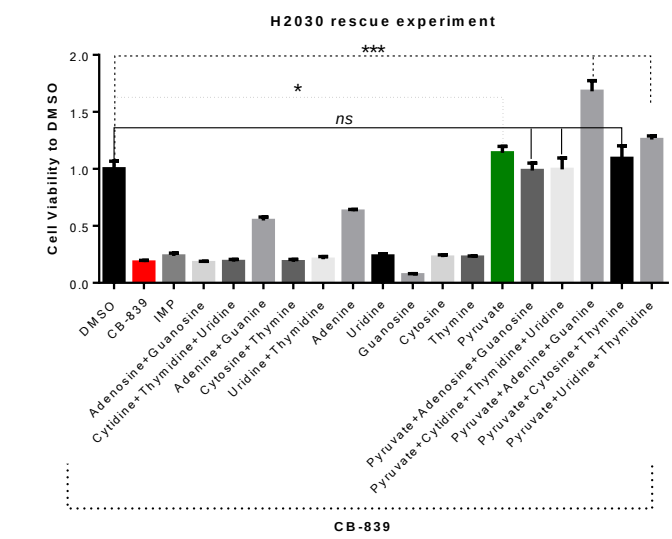
D
H2030 rescue experiment
Cell Viability to DMSO
ns
DMSO
CB-839
IMP
Adenosine+Guanosine
Cytidine+Thymidine+Uridine
Adenine+Guanine
Cytosine+Thymine
Uridine+Thymidine
Adenine
Uridine
Guanosine
Cytosine
Thymine
Pyruvate
Pyruvate+Adenosine+Guanosine
Pyruvate+Cytidine+Thymidine+Uridine
Pyruvate+Adenine+Guanine
Pyruvate+Cytosine+Thymine
Pyruvate+Uridine+Thymidine
CB-839

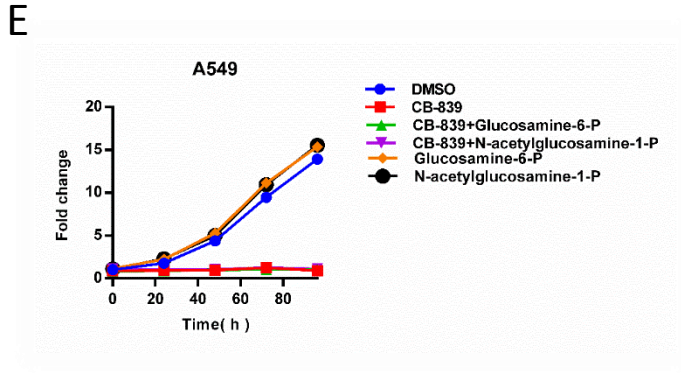
E
A549
Fold change
Time(h)
DMSO
CB-839
CB-839+Glucosamine-6-P
CB-839+N-acetylglucosamine-1-P
Glucosamine-6-P
N-acetylglucosamine-1-P

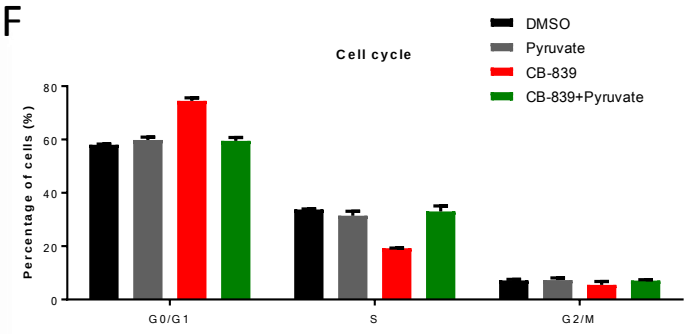
F
Cell cycle
Percentage of cells (%)
G0/G1
S
G2/M
DMSO
Pyruvate
CB-839
CB-839+Pyruvate

Figure S7. (A) Cell proliferation, assessed using the SRB assay, in isogenic LKB1 pairs of A549 cells with or without NRF2 knockdown, performed with different concentrations of glucose. **(B)** Glucose uptake rate after treatment with 1μM CB-839 in A549 control, KEAP1, or siNRF2 cells. **(C)** Cell viability of H2030 cells treated with 1μM CB-839 and **(D)** the indicated concentrations of exogenous nucleotides plus glycolysis and tricarboxylic acid intermediates. **(E)** Cell proliferation, assessed using the SRB assay, in A549 cells after treatment with 1μM CB-839 and hexosamine intermediates. **(F)** Cell cycle analysis of A549 cells at 24 hours after treatment with 1mM pyruvate, 1μM CB-839, and 1μM CB-839 plus 1mM pyruvate. All data are presented as mean ± standard error of the mean (error bars). A representative experiment is shown. Statistical significance: *$P \leq 0.05$; **$P \leq 0.01$; ***$P \leq 0.001$.